3D Hierarchical and Porous Layered Double Hydroxide Structures : an Overview of Synthesis Methods and Applications

3D Hierarchical and porous layered double hydroxide structures: an overview of synthesis methods and applications

Vanessa PREVOT[1,2], Yasuaki TOKUDOME[3]

[1]Université Clermont Auvergne Université Blaise Pascal, Institut de Chimie de Clermont-Ferrand, BP 10448, F-63000 Clermont-Ferrand, France.

[2]CNRS, UMR 6296, ICCF, F-63171 Aubiere, France.

[3]Department of Materials Science, Graduate School of Engineering, Osaka Prefecture University, Sakai, Osaka, 599-8531, Japan.

Abstract

Nanostructured layered double hydroxide (LDH) materials with unique diffusion properties, large surface area along with desired functionalities have recently been produced for a number of well-established and advanced fields of applications. In this review, we describe and discuss the main synthetic methods that have been reported for the fabrication of porous LDH with tailored chemical composition and porosity. The efficiency of soft and hard templating approaches is particularly reviewed. A special emphasis is put on the microstructure and porosity of the materials according to the synthetic method involved. Finally, the performance enhancement of the materials due to the presence of porosity, especially macroporosity, in applications such as pollutant removal, catalysis and energy storage and conversion is overviewed.

Keywords: Nanostructured materials, layered double hydroxides, porosity, template synthesis, hierarchical structures

1. Introduction

Within the emergence of wide range of potential applications, layered double hydroxides (LDH) attracted during these last two decades increasing attention not only from the academic researchers but also from industrial community [1-4]. These materials are chosen for their unique bidimensional layers, their capacity to adsorb, to intercalate, and to immobilize species of interest. LDH defined by the general formula $[M^{2+}_{1-x}M^{3+}_{x}(OH)_2]^{x+}$ $[(A^{n-})_{x/n}, yH_2O]$ (usually abbreviated as $M^{2+}M^{3+}$-A, where M^{2+} and M^{3+} are respectively divalent and trivalent metals, and A^{n-} represents the interlayer anion compensating the positive charge of the metal hydroxide layers), are synthetic layered compounds with positively charged brucite-like layers of mixed metal hydroxides separated by interlayer hydrated anions. The main intrinsic properties of this class of materials are their adsorption behavior, related to their high layer charge density, their anionic exchange capacity in the range of 200-400 mEq/100g, and swelling abilities. Moreover, LDH present the advantage to be easily prepared in laboratory, through economically viable soft chemical processes, in terms of pressure, temperature and pH. By finely tuning the synthetic parameters, a huge variety of chemical composition involving diverse metal cations and interlayer anions can be achieved. It is noteworthy that the formation of LDH is in competition with those of related hydroxide or hydrated oxides. Thermodynamic studies evidenced that LDH precipitation is favored due to their greater stability compared to the corresponding simple hydroxides [5]. However, usually peculiar attention should be paid to avoid precipitation of side phases and contamination of carbonate anion. Although fine tuning of the porosity is required to improve the LDH performance in various applications involving reactions at the interfaces such as adsorption, catalysis, energy conversion, it still remains considerably challenging. While many reviews, journal special volumes, and book chapters detail the general LDH preparation and applications [2-4,6,7], the present one will focus mainly on 3D hierarchical and porous LDH materials using examples of the recent literatures from their elaboration to the features of porous LDH which enhance the LDH efficiency in various fields of applications. In this review, we will first outline how synthetic strategies based on soft and hard templating approaches can be used to prepare LDH porous materials as summarized in Scheme 1. The subsequent section will illustrate how such porosity control can be used advantageously in LDH potential applications, such as adsorption, catalysis, energy production, storage and conversion.

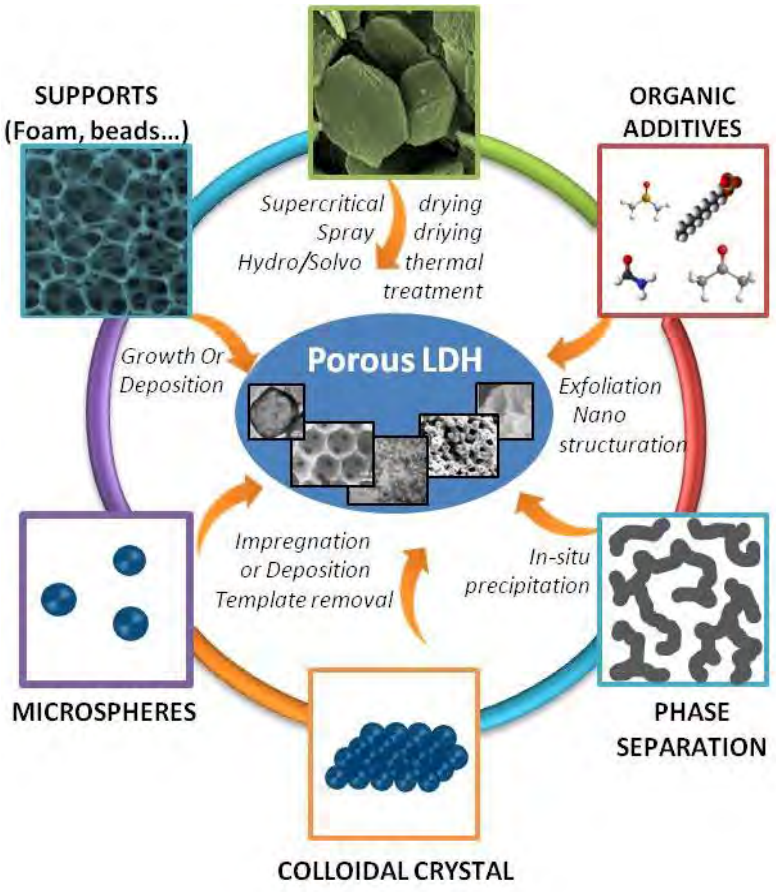

Scheme 1 Schematic representation of the main synthetic approaches to prepare porous LDH

2. Synthesis method towards porous LDH

2.1 Textual porosity as a result of aggregated crystals.

The most primitive strategy towards porous LDH relies on the porosity among aggregated LDH crystals. The so-called textural porosity is introduced as a result of interstices of aggregated crystals. Even though the pore size distribution obtained thereby is broad and the pores are not well-organized, textural pores can increase surface area and enhance the accessibility to crystal surface.

LDH with the textural porosity are synthesized by an alkalization reaction from a starting mixture of metal salts dissolved in an aqueous solvent. Typical examples of synthesis methods are reviewed below. Mg-Al LDHs with textural porosity were demonstrated to form via coprecipitation reactions. $NaOH/Na_2CO_3$ [8,9] or urea [10,11] works as an alkalization agent to precipitate LDH crystals from $MgCl_2 \cdot 6H_2O$ and $AlCl_3 \cdot 6H_2O$ at a relatively low temperature below 100 °C. Also, there has been reports on the synthesis of Ni-Al LDH [12], Co-Ni-Al LDH [13], Li-Al LDH [14] with textural porosity via hydrothermal and solvothermal methods, where high temperature and high pressure afford to yield LDH with a

relatively high purity. There have been some reports on the preparation of LDH hollow microspheres by optimizing crystallization, dissolution, and recrystallization of constituent crystals [15-17]. Activating the reaction steps of nucleation, crystal growth, and aggregation is a key to tune the textural porosity, and for this purpose, using sonication and/or adding ethylene glycol and glycine as a chelating agent have been employed [9,18,19]. The use of chelating agent also plays an important role to control structure and size of each crystals as well as the stability of crystals [20,21]. As a result, higher structural ordering is achieved in the presence of organic additives. Detailed discussion on this point is summarized in the section of *2.3 Soft Templating*. LDH with a textural property is usually obtained as powders, whereas also it can be prepared on substrates, such as graphene and metal plates, through inhomogeneous nucleation [22,23]. Ni foil, Al sheet, porous anodic alumina aluminum substrate, MXene nanosheets were successfully used to support *in-situ* LDH growth [24-29] by simple immersion into a metal salt solution in presence of precipitating agent (NaOH, NH_4OH, hexamethylenetetramine (HMT), urea…). Microstructures of LDH films can be easily tailored by the ion concentrations, the crystallization time and temperature. Zhang et al. further evidenced that during anion exchange reaction in presence of laurate anions, hollow hemispherical protrusions are generated at the film surface attributed to air bubble template mechanism [30].

Assembling exfoliated LDH nanosheets is another promising way to form textural porosity with a higher specific surface area compared to the pristine LDH. Although restacking of exfoliated nanosheets had been a critical drawback to achieve high porosity starting from exfoliated LDH nanosheets, O'Hare group recently developed a technique to avoid restacking with a technique named as the Aqueous Miscible Organic Solvent Treatment (AMOST) (Figure 1) [31,32]. This process forms a disordered card-house structure of LDH with a high porosity, achieving surface areas of 365 m^2/g and 458.6 m^2/g for Mg/Al-CO_3 [31] and Zn_2Al-borate LDH [32], respectively. Such a technique with exfoliated nanosheets allows to functionalize LDH as well as to introduce porosity, leading to enhance adsorption [33], mechanical [34], optical [35], magneto-optical [36,37], and electrochemical [38] properties.

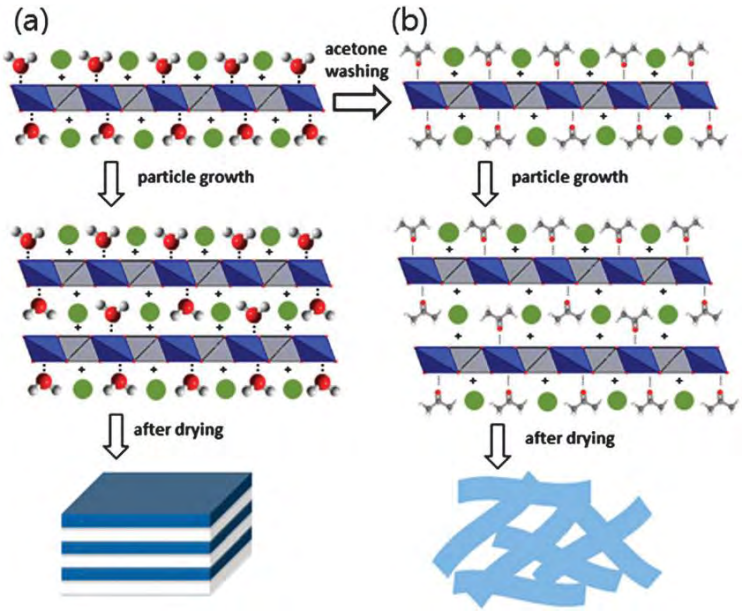

Figure 1 Proposed mechanism for the formation of (a) conventional LDH and (b) highly dispersed LDH by the AMOST method. Reproduced from Ref. [32] with permission from The Royal Society of Chemistry

2.2 Post-treatment

Different post-synthetic treatments can be applied to pre-synthesized LDHs to control the particle aggregation, allowing to tune the LDH textural properties and morphologies. Spray drying has been used in order to prepare spherical microsphere with a diameter in the micron range formed by LDH nanoparticle aggregation. Typically, a LDH colloidal suspension obtained either by polyol method [39] or separated nucleation and aging steps [40] is sprayed to form an aerosol which leads upon solvent evaporation to spherical microparticles [41,42]. Spherical morphology is maintained during anion exchange and calcination, allowing the preparation of hybrid LDH and mixed metal oxide microspheres. These latter were efficiently involved in photocatalytic degradation [43] and used as sacrificial template for chemical vapor deposition (CVD) growth of graphene and porous graphene microsphere formation [44]. In limiting the capillary forces which occur during drying, supercritical drying is well-known as an efficient process to produce highly porous aerogels [45]. LDH aerogels were produced using LDH wet physical gels by applying water exchange with a non-aqueous solvent and subsequent CO_2 supercritical drying [46,47]. Even if monoliths are not systematically obtained, such treatment induces a net increase of the mesoporosity compared to standard ambient drying. Post-treatments have been also applied to LDH dispersed within a polymer matrix allowing to produce macroporous nanocomposites. A hierarchical porous LDH polyacrylamide nanocomposite with pores in both micro- and nanometer scales was prepared

after freeze-drying of the hydrogel [48]. Electrospinning was also applied to a poly-ε caprolactone LDH nanocomposite to fabricate fibrous scaffolds [49]. LDH based nanocomposite foams were also reported involving *in-situ* polymerization process of polyurethane [50], and a high pressure CO_2 dissolution foaming process [51] of polystyrene, poly(styrene-co-acrylonitrile), and poly(methyl methacrylate). The *in-situ* coprecipitation of CoAl-LDH particles in the presence of exfoliated graphene oxide led to LDH nanosheet supported on graphene aerogel constructed by the physical cross-links between graphene sheets, via a one-step hydrothermal treatment assisted by a freeze drying process [52].

2.3 Soft templating

Soft-templating has been widely adopted to prepare mesoporous materials in alkoxide-derived sol-gel systems, where micelles of amphiphilic organic molecules (surfactants and water soluble polymers) are used to template well-defined mesoporous structures. Cooperative self-assembly between organic templates and inorganic precursors yield organized architecture and subsequent removal of organic templates by extraction or calcination create well-defined porosity. The structure of the mesophase depends on the packing properties of the surfactant molecules, and thereby structure of mesopores obtained by soft-templating is highly tunable by the nature of surfactant and composition of the starting mixture [53].

Considering that micelles represent colloidal dispersions with a particle size normally within 5 to 100 range [54], building blocks comprising mesowall are required to be small enough in nm range. The size of crystalline nanobuilding blocks used so far for the successful fabrication of well-ordered mesoporous structures is indeed less than 4-6 nm when pluronic surfactants (poloxamers) are used as soft templates [21,55,56]. For this reason, there are limited number of reports on the simultaneous achievement of well-defined periodic ordering of mesophase and crystallization of mesowall, such as organosilica [57], aluminosilicate [58], CeO_2 [56], γ-Al_2O_3 [59], and TiO_2 [60]. This requirement on the size of crystalline nanobuilding block imposes a primal challenge towards porous LDH via soft-templating because rapid crystallization kinetics of metal hydroxides, which typically form micron-scale crystals with a high crystallinity, prevents assembling them into an ordered mesophase. In addition, previous reports on mesoporous materials with crystalline wall typically involve a calcination step to crystallize precursory amorphous mesowall, whereas it cannot be applied to access to mesoporous hydroxides due to their lower thermal stability.

To date, there are various reports on the synthesis of porous LDH in the presence of

surfactant micelles. Gunawan et al reported the preparation of coral-like porous Mg-Al LDH microspheres in ethylene glycol/methanol/sodium dodecyl sulfate system (SDS) (Figure 2)[61].

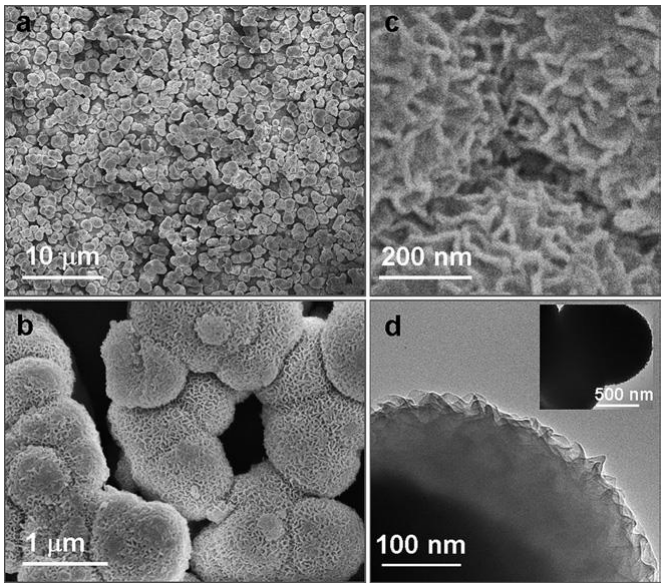

Figure 2 SEM and TEM images of SDS-intercalated Mg-Al LDH prepared in a mixture of EG and methanol of 1: 1 volumetric ratio at 150 °C for 18 h. Reproduced from Ref. [61] with permission from The Royal Society of Chemistry

A flower-like Mg-Al LDH porous microstructure was demonstrated with SDS by Zhang et al and Sun et al.[62,63]. Shao et al reported the preparation of Mg-Fe LDH microspheres with the morphologies of hollow, yolk−shell, and solid interior structure by a hydrothermal reaction in NaOH aqueous system with SDS additive [64]. Using SDS as structure directing agent allows to change interlayer distance as well as macro-morphology (aggregated state) of LDH crystals [62,63]. Additionally, SDS anions can tune zeta potential of LDH nanosheets, affording to construct composites, such as graphene/LDH nanosheets [65].

Surfactant additives for LDH structuration that are in most cases SDS, apparently work in the different way from well-known “soft-template” in alkoxide-derived systems. Pore size of LDHs are typically far larger compared to the size of micelles, and the formation of well-defined mesoporosity originated from surfactant micelles has not been clearly confirmed by characterization means of small angle X-ray scattering (SAXS) and N_2 adsorption. The organic surfactants and amphiphilic polymers rather work as nucleation sites [62,63] and/or an aggregation directing agent in macroscale [61]. Recently, successful soft-templating towards mesoporous LDH with using a nonionic surfactant (Pluronic F127) was achieved by limiting crystal growth and controlling aggregation [20]. Cooperative self-assembly between pluronuc F127 and LDH nanocrystals with the size as small as 8 nm was successfully

achieved (Figure 3). Further structural ordering of mesophase would be possible by reducing the size of crystals used as nanobuilding blocks.

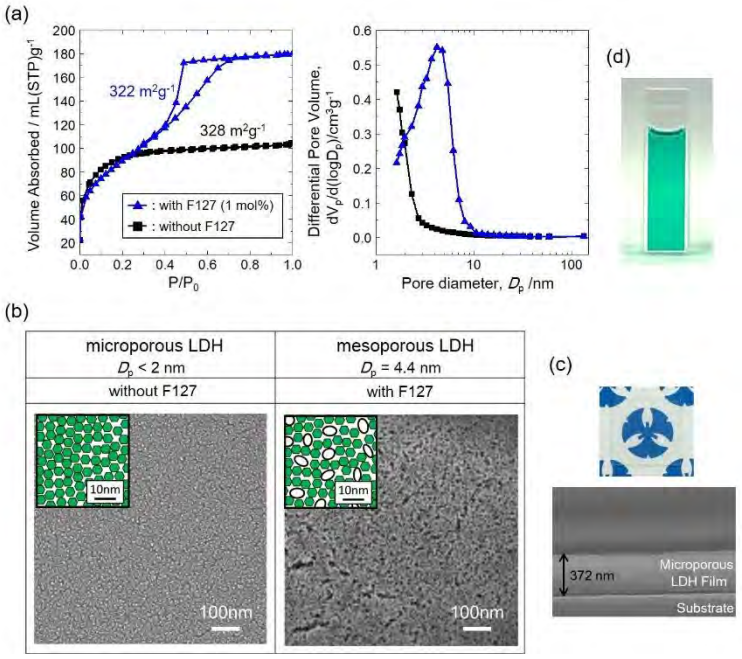

Figure 3 (a) N_2 sorption isotherms and corresponding BJH pore size distributions, (b) FE-SEM images of soft-templated mesoporous LDH films with and without F127 additive. (c) Optical and SEM images of a microporous LDH thick film. (d) Suspension of LDH nanocrystals used for the coating. Adapted with permission from [20] Copyright (2016) American Chemical Society.

Another strategy towards porous LDH in the presence of a polymer is the alkalization reaction accompanied with phase separation. Starting from an aqueous mixture of metal salts, alkalization reaction induced by propylene oxide (PO) can crystalize LDH [66]. A homogeneous and fast pH increase is induced through the epoxide ring-opening reaction with the nucleophilic species [67]. Along with the pH increase, cationic species are consumed by the nucleation and growth of nanocrystals to form monolithic wet gel of hydroxides. The PO-mediated alkalization was demonstrated to be coupled with phase-separation phenomena, resulting in well-defined hierarchically porous structures [68]. Tokudome et al. demonstrated the synthesis of hierarchically porous Mg-Al LDH via PO-mediated alkalization accompanied with phase separation (Figure 4) [69]. Monolithic LDH materials with hierarchical pores in μm and nm ranges can be obtained via an aqueous one-pot reaction at as low as 40 °C. This synthesis method exhibits compositional versatility and applicable to the preparation of $M^{2+}_{1-x}Al_x(OH)_2Cl_x$ (M^{2+}: Mg^{2+}, Mn^{2+}, Fe^{2+}, Co^{2+}, Ni^{2+}, Cu^{2+}, Zn^{2+}) with hierarchically porous structures [70].

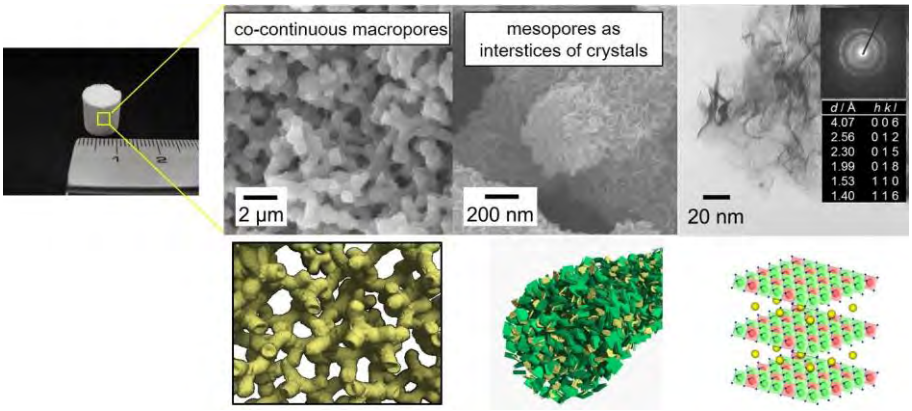

Figure 4 Hierarchically porous Mg-Al LDH monolith obtained through phase-separation accompanied with sol-gel transition [69].

2.4 Supported LDH synthesis

An interesting approach growing quite rapidly to produce LDH based hierarchical architectures is the use of 3D supports (Figure 5). Thanks to their positively charged surface covered by hydroxyl groups, LDH can easily interact with many kind of materials. As previously described in the case of 2D substrates, this approach allows a preferential orientation of LDH particles [25,29,71] and the preservation of morphology and/or macroporosity of the modified support.

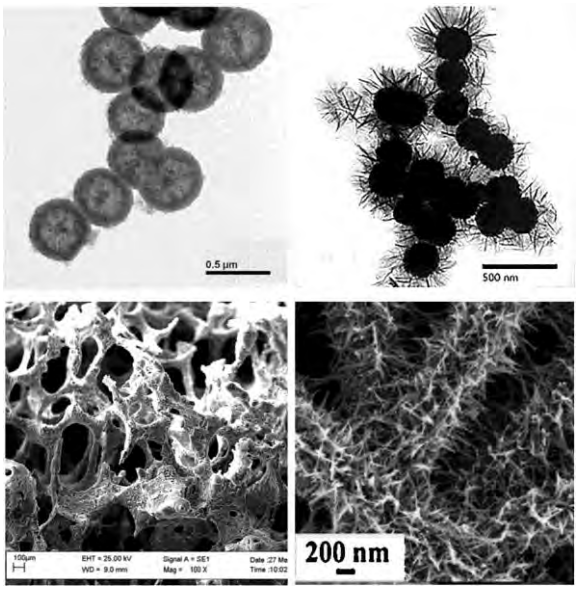

Figure 5 LDH supported on hollow mesoporous silica [72], Fe_3O_4 spheres [73], FeCr alloy foam [74] and carbon nanofibers [75]. Adapted with permission from [72]. Copyright (2016) American Chemical Society. Reprinted from [74,75], Copyright (2016), with permission from Elsevier. Reprinted from [73], Copyright (2016), with permission from John Wiley and Sons.

Two main synthetic strategies can be distinguished to achieve the LDH deposition on supports either by the *in-situ* coprecipitation of LDH over the surface or by the self-assembly of

preformed LDH nanoparticles at the surface. Table 1 summarized the main methods reported for preparing LDH on various kinds of supports. In one hand, to perform the *in-situ* coprecipitation of LDH, well-known synthetic methods reported for standard LDH synthesis such as, classical coprecipitation in presence of basic agent, coprecipitation using homogenous precipitation (involving retardant base ***i.e.*** urea, HMT…), electrosynthesis, or induced hydrolysis, are usually carried out in presence of the structured supports. Hydrothermal or solvothermal treatments can be associated to promote the crystal growth and tune the morphology of LDH coating. Typically, a selected support is introduced in an aqueous solution of mixed metal salts containing divalent and trivalent metal cations. Then, the adequate pH range for the LDH formation by coprecipitation is reached either by NaOH addition, thermal decomposition of a retardant base, or nitrate reduction. For instance, Abushrenta et al. reported the preparation of hierarchical CoAl LDH arrays by coprecipitation using urea in the presence of a $Co(OH)_2$ supported on macroporous Ni foam. A subsequent alkaline etching induced a partial Al removal producing mesoporous LDH layers. Due to an enhancement of the charge transport and short ion diffusion, such hierarchical architecture appeared as promising supercapacitors [76]. It is noteworthy that the support can act as a metal cation precursor through partial hydrolysis and contributes to the final LDH chemical composition. This is the case, for instance in the presence of Al_2O_3 spheres [77,78] or biomorphic aluminum based fibers [79-81]. The *in-situ* growth of LDH nanoparticles vertically on the 3D support is an interesting strategy compared to platelet stacking, leading to macroporous structure.

In another hand, pre-synthesized LDH nanoparticles or exfoliated LDH nanosheets can also be deposited on the 3D support surface taking advantages of the LDH positively charge layers allowing electrostatic interaction with negatively charged supports. In this approach LDH coating is achieved either by simple deposition, by layer-by-layer process or by electrophoretic deposition (Table 1).

Using a self-assembly approach, hollow mesoporous silica spheres were successfully coated with exfoliated CoAl LDH and graphene oxide by alternate adsorption of nanosheets and subsequent chemical reduction to generate SiO_2/LDH/graphene hierarchical structure [72]. Obviously, a large variety of supports were reported including oxide microspheres (Al_2O_3, Fe_2O_3, Fe_3O_4, MnO_2…), nanowires (CuO, Al, Ag), metal foams (FeCr alloy, Ni), macro/meso alumina and silica, minerals such as zeolites, sepiolite and vermiculite, carbon nantubes, 3D carbon oxide foam, carbon fibers, polymer foams or electrospun fibers, cellulose fibers and hierarchical carbon obtained by biotempate calcination. Interestingly the final composite

materials benefits from the support morphology and intrinsic properties that is especially the case in using magnetic or conductive support such as iron oxides, metallic foams or carbon.

Table 1 3D hierarchical nanostructured LDH synthesized using various supports

Method	Metal salts/ precursor composition	Precipitating agent	Conditions	Support	Ref
Co-precipitation	$Ni(NO_3)_2$, $Fe(NO_3)_3$	NaOH/ Na_2CO_3	65°C/6h	MnO_2 spheres	[82]
	$Mg(NO_3)_2Cu(NO_3)_2$, $Al(NO_3)_3$	NaOH/Na_2CO_3	65°C/36h	Fe_3O_4	[83]
	$Mg(NO_3)_2$,$6H_2O$ $Al(NO_3)_3$	NaOH/Na_2CO_3	60°C/24h	Fe_3O_4	[73]
	$Mg(NO_3)_2$ or $Ni(NO_3)_2$, $Al(NO_3)_3$	NaOH/Na_2CO_3	RT/ 15 min	Fe_3O_4	[84]
	$MgSO_4$ $Al_2(SO_4)_3$	NaOH	RT	Ti discs	[85]
	$Ni(NO_3)_2$;$CoCl_2$	-	180°C/ 24h	Ni foam	[86]
	$Mg(NO_3)_2$,$Al(NO_3)_3$	NaOH, Na_2CO_3	2h, RT	Zeolite	[87]
	$MgCl_2$;$AlCl_3$	NaOH	4h, RT	Sepiolite	[88]
	$FeSO_4.Fe_2(SO_4)_3$	NaOH, Na_2CO_3	-	Sepiolite	[89]
	$Ni(NO_3)_2$; $Co(NO_3)_2$; $Mn(NO_3)_2$	NaOH, Na_2CO_3	RT, 24h	MWCNT	[90]
	$ZnCl_2$, $AlCl_3$	NaOH	RT, 24h	Cellulose	[91]
	$Zn(NO_3)_2$, $Al(NO_3)_3$	NaOH Urea	100°C, 2h	Cellulose	[92]
Retardant Base	$Ni(NO_3)_2$;$Al(NO_3)_3$	Urea	HT 95°C/ 24h	Ag nanowire	[93]
	$Ni(NO_3)_2$;$Al(NO_3)_3$	Urea	HT 120°C/12h	Ni foam	[94]
	$Co(NO_3)_2$;$Al(NO_3)_3$	Urea	HT 120°C/6h	Ni foam	[95]
	$Co(NO_3)_2$; $Al(NO_3)_3$	Urea	HT 100°C/ 24h	$Co(OH)_2$/ Ni foam	[76]
	$Fe(NO_3)_3$	Urea	HT 100°C/ 8h	$Co_2(OH)_2CO_3$/Ni foam	[96]
	$Mg(NO_3)_2$; $Al(NO_3)_3$	Urea	HT 120°C/ 24h	Vermiculite	[97]
	$Ni(NO_3)_2$;$Al(NO_3)_3$	Urea	HT 100°C/24h	GO nanocups	[98]
	$MnCl_2$; $NiCl_2$	HMT	HT 90°C/6h	Graphene sponge	[99]
	$Co(NO_3)_2$ $FeCl_2$	HMT/I_2	HT 100°C/3h	Carbon fiber cloth	[100]
	$Co(NO_3)_2$; $Al(NO_3)_3$	Urea	HT 90°C/ 6h	Carbon fibers	[101]
	$Ni(NO_3)_2$; $Co(NO_3)_2$	Urea or HMT	80°C/ 6h	Electrospun carbon nanofibers	[75]
	$Zn(NO_3)_2$; $Al(NO_3)_3$	Urea	HT 120°C/10h	$ZnCo_2O_4$	[102]
	$Mg(NO_3)_2$; $Al(NO_3)_3$	Urea	HT 120°C/24h	Electrospun PVDF	[103]
	$Mg(NO_3)_2$; $Al(NO_3)_3$	Urea	HT 100°C/ 8h	Electrospun PAN/PMMA	[104]
Electrosynthesis	$Co(NO_3)_2$; $Fe(SO_4)$	Nitrate reduction	-1.0V, 0- 200s	CuO@Cu nanowire	[105]
	$Ni(NO_3)_2$; $Fe(NO_3)_3$	Nitrate reduction	-0.1 mA/cm^2 50-400s	WO_3 nanorod	[106]
	$Ni(NO_3)_2Al(NO_3)_3$	Nitrate reduction	-0.9 V/ -1.2V 600-1800s	FeCr alloy foam	[74]
	$Mg(NO_3)_2$; $Al(NO_3)_3$ $Rh(NO_3)_3$	Nitrate reduction	-1.2 V 2000 s	FeCr alloy foam	[107]
	$Ni(NO_3)_2$; $Fe(NO_3)_3$	Nitrate reduction	-1.0 V, 300s	Ni foam	[108]
	$Ni(NO_3)_2$/$Co(NO_3)_2$/$LiNO_3$ $Fe(SO_4)$	Nitrate reduction	-1.0 V, <300 s	Ni foam	[109]
	$Ni(NO_3)_2$;$CoCl_2$	Nitrate reduction	-1.0 V, < 200 s	PPy nanowire/Ni foam	[110]
Induced hydrolysis	$Ni(NO_3)_2$	NH_4OH	100°C/ 48h	Fe_3O_4@SiO_2@AlOOH	[111]
	$Co(NO_3)_2$; $Cu(NO_3)_2$,	NH_4OH	HT 120°C/ 18h	Al_2O_3 microspheress	[77]
	$Mg(NO_3)_2$	HMT	HT 120°C/12h	Al_2O_3/carbon fibers	[112]
	$MgSO_4$	HMT	HT 120°C/10h	Al_2O_3/C microspheres	[113]
	$Mg(NO)_3$	Urea	HT 90°C/ 24h	θ-Al_2O_3 spheres	[78]
	$Mg(NO_3)_2$; $Ni(NO_3)_2$	NH_4NO_3, NH_3	150°C/ 12h	Al Wire	[114]
	$Ni(NO_3)_2$, Co porous coordination polymer	-	Ethanol reflux 1h	Melamine polymer foam	[115]
	$CaCl_2$	Urea	150°C/3d	Mesoporous alumina	[116]
	$Mg(NO_3)_2$;$Ni(NO_3)$; $Co(NO_3)_2$	Urea	120°C/ 24h	Macroporous γ–Al_2O_3	[117]
	$Mg(NO_3)_2$;$Al(NO_3)_3$	-	600°C/6h HT rehydration	SBA-15	[118]

	$Mg(MeO)_2$	-	450°C/15h HT 125°C/21h	Meso-macro Al-SBA-15	[119]
	MgAl-, ZnAl-, NiAl-	HMT/Urea	75°C-140°C 10h	Biotemplated Al_2O_3	[80,120, 121]
	$Ni(NO_3)_2$	Urea	HT 100°C/24h	AlOOH/ Carbon NS	[79]
	$Ni(NO_3)_2$	NH_4OH	75°C/20h	AlOOH/C cloth	[122]
Alternate deposition	Co_2Al- and Graphene oxide		Formamide	Hollow mesoporous SiO_2 spheres	[72]
Electrophoresis	MgAl-	-	1V- 20V	Tubular α-alumina	[123]
	Mg_3Al- Ca_3Al-	-	40V – 60 min	Activated carbon fiber cloth	[124]
Layer by Layer	MgAl- NiAl-	-	Alginate and chitosan	Polyurethane foam	[125]

2.5 Use of sacrificial template

An alternative strategy to generate porous LDH is to use a sacrificial template which can be easily eliminated in a subsequent step. Usually in the first step, the LDH phase is associated to the sacrificial template following similar strategies as previously described for supported LDH. In the second step, the support is eliminated by dissolution or combustion leading to LDH porous structure. The different sacrificial templates and the LDH deposition methods used are listed in Table 2.

Table 2 Porous LDH obtained by sacrificial templating approach.

Sacrificial template	LDH composition	Method	Removal technique	Ref
SiO_2	MgAl-, NiAl	Induced hydrolysis	Basic dissolution	[126]
SiO_2	MgAl-	*In-situ* coprecipitation	pH 11, 40°C	[127]
Hollow SiO_2	CoAl-	Layer-by-layer	Extraction	[72]
Carbon nanospheres	MgAl-	Self-assembly	Calcination 500°C	[128]
Carbon nanosphere	NiAl-	*In-situ* template formation	Calcination	
Carbon Hollow microsphere/ SiO_2	NiAl-	Induced hydrolysis	Etch process	[129]
γ-AlO(OH)/Carbon fiber	MgAl-	Induced hydrolysis	Calcination 500°C 1h	[130]
PS spheres	CoFe- NiAl-	Self-assembly	Calcination 700°C 4h	[131]
PS spheres	MgAl-	Layer-by-layer	Calcination 480°C 4h	[132]
PS array	NiAl-	Nanoparticles infiltration	Dissolution	[20]
PS array	NiAl-	Electrosynthesis	Dissolution	[133, 134]
PS array	MgAl-	Successive impregnation	Calcination or dissolution	[135-141]
Legumes	ZnAl-	Induced hydrolysis	Calcination 500°C/6h	[142]

An elegant alternative to produce porous networks was reported by Xiang et al., where the LDH crystallization and glucose carbonization is simultaneously induced under hydrothermal conditions [143]. Carbon nanospheres are formed conjointly with LDH and removed from the composite by thermal decomposition to generate mesoporous mixed metal oxides.

By this approach, the preparation of hollow LDH spheres [126,127,129,132,144], hollow LDH nanofibers [120,130,142] and 3D macro/mesoporous frameworks [134,135,137-139,141] have been reported (Figure 6). It should be remained that when sacrificial template is removed by calcination at a moderate temperature, layered mixed oxide is thermally crystalized in a certain extent with pristine LDH structure [2].

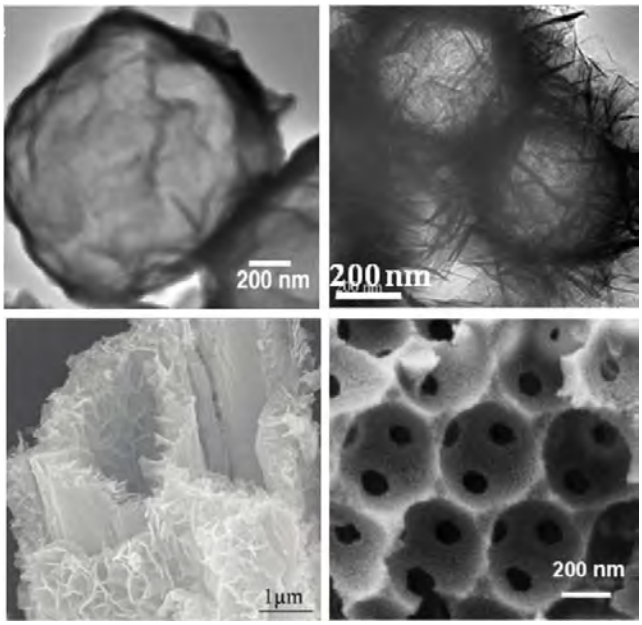

Figure 6 Hollow spheres, hollow fibers and 3D ordered macroporous LDH structure obtained using sacrificial template. Reproduced from Ref. [132] with permission from the Royal Society of Chemistry. Adapted with permission from [126,139,142] Copyright (2016) American Chemical Society.

As illustrated in this part, synthetic efforts were focused on the preparation of porous LDH structure to enhance accessibility, diffusion within the materials and mass transport. Table 3 gathered the textural properties reported for some of the previously described morphologies demonstrating that both mesoporosity and macroporosity can be successfully created. Since playing on the pore networks was reported as an efficient approach to improve the material performances, the advantages/effects of 3D hierarchical and porous LDH nanostructure in various fields will be detailed in the following part.

Table 3 Summary of textural properties of various porous LDHs.

Method	Composition	Morphology	Surface area (m^2/g)	Macropores	Ref
Urea hydrolysis	$ZnAlCO_3$	Hollow spheres	64	ND*	14
Ethylene glycol	$MgAlCO_3$	Microspheres	165	ND	9
Organic solvent treatment	$MgAl\text{-}CO_3$	Aggregated particles	365	ND	31,32
Spray dried	$MgAlCO_3$	Microspheres	-	87.9 nm	42
	NiAlAcetate		72	ND	41
	$MgAl\text{-}CO_3$		48	ND	44
	$ZnAlCO_3$		103	ND	43
CO_2 supercritical drying	$MgAlCO_3$ $NiAlCO_3$	Aerogel	305	ND	47
Pluronic F127	NiAlCl	Mesoporous film	322	ND	20
Phase separation	MgAlCl	Hierarchically porous monolith	238[1]	0.52 mm	69
Spherical template	MgAl-Ibuprofen	Hollow spheres	54	ND	128
Inverse opals	$MgAlCO_3$	3DOM[2]	42	0.64 mm	139

*ND : not determined [1]Sample calcined at 500°C [2]3-dimensionally ordered macroporosity

3. Field of applications of porous LDH

Porous LDH have been promising materials for various specific applications, taking advantage of high surface area and rapid molecular diffusion through interconnected pores (channels), as well as pristine surface properties of LDH crystals, such as hydrophilicity, positive electric-charge, and intercalation/deintercalation capability. Typical application fields of porous LDHs are briefly reviewed in this section.

3.1 Adsorption and removal for purification and environmental purposes

Table 4 Adsorption on porous LDH

Adsorbate	LDH composition	Porosity of synthesized LDH	Adsorption capacity	Enhancement (vs standard LDH)	Ref
Orange II	MgAl-	Inverse opal	4.34 mmol·g^{-1}	× 8.5	[137]
methyl orange	ZnAl-	Hierarchical textual porosity	248 mg·g^{-1}	× 1.4	[15]
methyl orange	NiAl-	Hollow nanowires	210 mg·g^{-1}	–	[16]
pyranine	MgAl-	Cocontinuous Hierarchically porous	1.8 mmol·g^{-1}	× 3.5	[69]
Congo red	MgAl-	Hierarchical textural	447 mg·g^{-1}	Comparable to activated carbon	[130]
Congo red	Ni/Mg/Al-	Flower-like hollow microspheres	1250 mg·g^{-1}	× 2.1 of MgAl-LDH flakes	[146]
Cr(VI)			103 mg·g^{-1}	× 6.7 of ZIF-67 microcrystals	
Phosphate	Zn/Al-	Hollow microspheres	232 mg·g^{-1}	–	[17]
F^-	Li/Al-	Hierarchical textural porosity	159 mg·g^{-1}	–	[14]
F^-	Zn/Al-	LDH supported on cellulose	25.2 mg·g^{-1}	× 2–4	[91]
$S_2O_3^-$	Ni/Al-	Grown on Ni foam	209 mg·g^{-1}	–	[94]

Table 4 shows the relationship between adsorption capacities and pore characteristics of porous LDH. Previous reports in the list successfully demonstrated advantages/improvements by the introduction of porosity into LDH materials. High loading of adsorbates on porous LDH has been demonstrated for anionic dye molecules, such as orange II [137], methyl orange [15,16], pyranine [69,145] and Congo-red [130], where various porous morphologies, including hollow spheres [15], hollow nanowires [16], 3D ordered macroporous [137], hierarchically-porous monolith [69], microtubes [130], and urchin-like particles [146], have been employed. The transport of molecules in porous LDH primarily depends on the macropores (macrochannels) and the introduction of larger macropores accelerates adsorption kinetics more progressively [145]. Whereas the introduction of mesopores, increases loading capacity at an equilibrium state [145]. There has been various reports on the application of porous LDH towards environmental purposes, targeting at harmful anionic species in waste water, such as phosphates [17], various oxyanions (SO_4^{2-}, CrO_4^{2-}, MoO_4^{2-}, HVO_4^{2-}) [70], and fluoride ion [14,91], thiosulfate [94], arsenic [89], and chromium(VI) oxyanion [97]. Porous

LDH have been also used for the extraction of phenolic compounds [135], and oil separation from oil-polluted water [104].

3.2 Energy production, storage and conversion

Highlighted electrochemical properties of porous LDH-base electrodes are listed in Table 5. LDH have been widely applied as electrode materials due to their high theoretical specific capacitance, high redox activity, low manufacturing cost, and environmental-friendly nature. The enhancement of capacitance of LDH electrodes has been achieved by the introduction of textured pores [12,23,100], and hierarchical porosity [76]. The capacitance of LDH-based electrodes was reported to be further enhanced by compositing LDH with carbon-based field of application that Ni foam can be used as Ni metal source as well as conductive substrate to produce a metal hydroxide electrode [148]. This technique allows one-step method to fabricate Ni-Al LDH electrode and is widely applied for the electrochemical applications of

Table 5 Electrochemical properties of porous LDH-based electrodes

Porous LDH employed	Highlighted properties	Ref
Flowerlike hierarchically porous Ni/Al-LDH	*C_s = 477 F· g^{-1} at J =12 A· g^{-1}	[12]
3D porous NiAl-LDH grown on graphene	C_s = 1256 F· g^{-1} at J = 1 A· g^{-1} C_s = 756 F· g^{-1} at J = 6 A· g^{-1}	[23]
CoFe-LDH nanosheets grown on carbon fiber	C_s = 774 F· g^{-1} at J = 1 A· g^{-1}, 91% retention of the initial C_s after 5000 cycles at J = 2 A· g^{-1}	[100]
$Co(OH)_2$@porous LDH grown on Ni foam	C_s = 1734 F· g^{-1} at J = 5 mA· cm^{-2}, 85% retention of the initial C_s after 5000 cycles at J = 5 mA· cm^{-2}	[76]
CoAl-LDH/graphene oxide/ MnO_2 nanocomposite with mesoporosity	C_s = 340-560 F· g^{-1} at J = 2 A· g^{-1}	[11]
$NiCo_2S_4$ nanotube@NiMn-LDH/graphene sponge	C_s = 1740 and 1268 mF· cm^{-2} at J = 1 and 10 mA· cm^{-2}, respectively, 84.5% retention after 5000 cycles	[99]
3D porous CoAl-LDH/graphene aerogel	C_s = 640 and 305 F· g^{-1} at J = 1 and 20 A· g^{-1}, respectively, 97% retention after 10000 cycles	[52]
NiCo-LDH supported on Ni form	C_s = 2682 F· g^{-1} at J = 3 A· g^{-1}, energy density of 77.3 Wh· kg^{-1} at 623 W· kg^{-1}	[86]

*C_s: specific capacitance; J: current density

LDH materials [86].

From different application aspects, noteworthy remarks and highlights on using porous LDH

in catalysis, bio, and others are summarized in Table 6 We will briefly go through in the following sections.

3.3 Catalysis

The introduction of porosity increases surface area and thereby enhances the catalytic activity of LDH-based materials. Some examples of the improvement of activity/selectivity in catalytic applications are listed in Table 6. For example, Halma et al reported that oxidation of heptane exhibits selectivity for the alcohol product over iron porphyrins accommodated in LDH with macroporous structure [140]. The authors explained that the reaction selectivity was impacted by the structure of LDH support with channel and micro-environments which can create a suitable structure for the access of substrates toward the reaction sites. Various catalytic reactions, such as alcohol oxidation [140], aldol condensation [118], ethanol electrooxidation [64], pollutant photodegradation [136] and photoelectrochemical water splitting [106], have been reported for porous LDH catalysts. Nanostructured LDH (nanoarray and nanoflakes) prepared on a Ni foam were also employed as electrocatalysts of oxygen evolution reaction (OER) [96,127,149]. A porous hydroxide showing OER activity was also prepared by selective etching of M(III) in hydroxide sheets [150]. In addition, mesoporous oxides with well-defined porosity have been used as a support to load catalytic LDH crystals; LDH precipitated on mesoporous AlOOH was used for selective hydrogenation [78] and as CO_2 adsorber after calcinations [116].

Table 6 Summary of catalytic, bio-, and other applications of LDH

Application	Composition and role of LDH	Porosity of LDH	Highlights, remarks, comparison with standard LDH	Ref
Catalysis	Host material (MgAl-)	3D ordered macropores	Reaction selectivity imparted by the macroporosity	[140]
Catalysis	Electroactive material (MgFe-)	Hollow microspheres	Electrocatalytic oxidation of ethanol achieved in alkaline fuel cell	[64]
Photolysis	Host material (MgAl-)	3D ordered macropores	Enhanced reaction kinetics due to the macroporosity	[136]
Photoelectrochemical water splitting	Co-catalyst (NiFe-)	Nano LDH flakes on WO_3 nanorod arrays	Benefit for light absorption and migration of carriers,	[106]
Electrocatalytic water splitting	Precursor (NiGa-)	Porous nanosheets	Selective etching of LDH to prepare porous hydroxide and chalcogenides	[150]
Hydrogenation	Catalyst support (MgAl-)	LDH-modified porous alumina	Higher catalytic activity/selectivity compared to standard	[78]
Amperometric detection of H_2O_2	Host material (MgAl-)	Textual pores	Detection limit of 1.5×10^{-8} M, sensitivity of 37 A· $M^{-1}cm^{-2}$	[151]
Trypsin adsorption	Adsorbent (MgAl-)	Aerogel with textural porosity	20 times higher adsorption capacity than conventional LDH	[47]
Bovine serum albumin adsorption	Adsorbent (MgAl-)	Aerogel with hierarchical porosity	>14 times higher adsorption capacity than standard LDH	[46]
Controlled drug release	drug release media (MgAl-)	LDH on porous titania	Pores prevent premature detachment of the LDH coating.	[85]
Controlled drug release	Host material (Mg/Al-)	Hollow microspheres	Better dispersion in the liquid phase and higher surface area	[128]
Non-enzymatic glucose sensor	Redox mediator (NiAl-)	3D macroporous LDH on carbon cloth	14.13 mA mM^{-1}· cm^{-2}, response time less than 1 s	[122]
Glucose biosensor	Enzyme support (NiAl-)	3D ordered macropores	×1.4 enhancement of sensitivity due to the macroporosity	[134]
Tissue engineering scaffold	Nanofiller (MgAl-)	Grown on 3D porous polymer	Improved the tensile strength, elongation, and proliferation and differentiation of cells	[49]
Li-ion battery	Electrode material ((Zn/Cu)Al-)	Interconnected nano -sheets with porosity	LDH-derived oxides exhibit higher capacity & better stability than pure ZnO	[22]
Photocatalysis	Adsorbent/catalyst (ZnAl-)	Textural porosity	Hierarchical structure improve the adsorption and photocatalytic properties	[102]
Fire suppression	Fire extinguishing agent (MgAl-)	Porous microspheres	Higher efficiency in suppressing gasoline pool fire	[9]
Superhydrophobicity	Microstructure (NiAl-)	Hexagonal micro-structures	Allow to immobilize lauric acid on rough surface to show contact angle of 163°	[24]
Electrochromic	Inverse opal (NiAl-)	Chromophore	Improvements in the electrochromic properties (×4 lager color change)	[133]
Antireflection coating	Porous film (MgAl-)	Switchable porous material	AR properties switchable by the reconstruction effect of LDH	[71]
NO_x Sensing	Sensor (MgAl-)	Hierarchical flower-like LDH	Response in 1.3 s and recovery time of 30 s to 100 ppm NO_x	[63]

3.4 Bio-applications

LDH have been investigated as biocompatible host materials due to the possibility of providing a suitable microenvironment for biomolecules, such as proteins and enzymes [151]. The introduction of porosity, especially large mesopores and/or macropores, can increases the

surface area which is accessible by large biomolecules with tens nm in size. High-density protein loading on porous LDH was reported for trypsine [47] and bovine serum albumin (BSA) [46,121], where enhancement of adsorption were reported as 20 times and 14 times compared to those for standard LDH, respectively (Table 6). There has been also various reports on loading and releasing an antibiotic [85], drug [128], enzyme [47], glucose biosensor development [122,134] and tissue-engineering scaffolds [49].

3.5 Others

Porous LDH materials have been used as precursor for porous metal oxides. For example, porous ZnO/$ZnAl_2O_4$ crystalized from Zn-Al LDH exhibit excellent cycling stability as an anode material for Li-ion batteries [22] and enhanced adsorption and photocatalytic properties toward Congo red [102]. Also, there are reports on the applications of porous LDH for fire suppression [9], designing superhydrophobic surface [24], electrochromic coating [133], erasable antireflective [71], and gas sensors [63]. For all these applications, the introduced porosity play important roles to generate respective properties (Table 6).

4. Concluding remarks

Over the last decade, 3D hierarchical and porous LDH has gained an increasing interest allowing the preparation of nanostructured LDH materials which displayed real advantages for various applications such as adsorption for environmental purposes, energy production, storage and conversion, photo, electro- catalysis and biosciences. Even if their synthesis is often challenging, the large panel of LDH synthetic pathways using soft chemistry conditions allowed to successfully design various LDH systems. For a given nanostructure, porous and hierarchical LDH materials may provide multifunctional properties by acting as a passive or an active host material with high surface area allowing to accommodate other components within the nanostructure or at the wall surface. By this way, nanostructured mutlicomponent systems can be achieved opening new opportunity for the applications of LDH-based

materials thanks to the functionality of accommodated component as well as advantages of pristine LDH, such as a rapid mass or charge transport. Based on the state of the art, the authors strongly believe that in a near future, even more complex LDH based porous assemblies may be designed displaying well-defined architectures of highly-controllable size with a better level of understanding of the synthesis-structure-properties relationship. A method of preparing porous LDH monoliths displaying good mechanical and thermal properties will be also necessary to open the way to actual applications.

Acknowledgement

Financial support from JSPS-MAE SAKURA program is gratefully acknowledged.

References:

1. Costantino U, Leroux F, Nocchetti M, Mousty C (2013) LDH in physical, chemical, bio-chemical and life science. In: Faiza Bergaya GLE (ed) Handbook of Clay Science. Elsevier Amsterdam, The Netherlands, Chapter 6, pp 765-791. Volume 765 Techniques and Applications
2. Forano C, Costantino U, Prevot V, Taviot Gueho C (2013) Layered Double Hydroxides. In: Faıza Bergaya GL (ed) Handbook of Clay Science, vol 5, Part A. Elsevier, Amsterdam, pp 745-783. doi: 10.1016/B978-0-08-098258-8.00025-0
3. Duan X, Evans DG, Editors (2006) Layered Double Hydroxides, Struct. Bonding, 119. Springer, Berlin/Heidelberg
4. Rives V (2001) Layered Double Hydroxides: Present and Future. Nova Science, New York
5. Costa DG, Rocha AB, Diniz R, Souza WF, Chiaro SS, Leitao AA (2010) Structural Model Proposition and Thermodynamic and Vibrational Analysis of Hydrotalcite-Like Compounds by DFT Calculations. J Phys Chem C 114:14133-14140. doi: 10.1021/jp1033646
6. Wang Q, O'Hare D (2012) Recent Advances in the Synthesis and Application of Layered Double Hydroxide (LDH) Nanosheets. Chem Rev 112 (7):4124-4155. doi:10.1021/cr200434v
7. Gu Z, Atherton JJ, Xu ZP (2015) Hierarchical layered double hydroxide nanocomposites: structure, synthesis and applications. Chem Commun 51 (15):3024-3036. doi:10.1039/c4cc07715f
8. Carja G, Nakamura R, Aida T, Niiyama H (2001) Textural properties of layered double hydroxides: Effect of magnesium substitution by copper or iron. Microporous Mesoporous Mater 47 (2-3):275-284. doi:10.1016/S1387-1811(01)00387-0
9. Ni X, Kuang K, Jin X, Xiao X, Liao G (2010) Large scale synthesis of porous microspheres of Mg-Al-layerd double hydroxide with improved fire suppression effectiveness. Solid State Sci 12 (4):546-551. doi:10.1016/j.solidstatesciences.2010.01.003
10. Xiao T, Tang Y, Jia Z, Li D, Hu X, Li B, Luo L (2009) Self-assembled 3D flower-like Ni^{2+}-Fe^{3+} layered double hydroxides and their calcined products. Nanotechnology 20 (47). doi:10.1088/0957-4484/20/47/475603
11. Gu TH, Gunjakar JL, Kim IY, Patil SB, Lee JM, Jin X, Lee NS, Hwang SJ (2015) Porous Hybrid Network of Graphene and Metal Oxide Nanosheets as Useful Matrix for Improving the Electrode Performance of Layered Double Hydroxides. Small 11 (32):3921-3931. doi:10.1002/smll.201500286
12. Song Y, Wang J, Li Z, Guan D, Mann T, Liu Q, Zhang M, Liu L (2012) Self-assembled hierarchical porous layered double hydroxides by solvothermal method and their application for capacitors. Microporous Mesoporous Mater 148 (1):159-165. doi:10.1016/j.micromeso.2011.08.013

13. Li S, Mo S, Li J, Liu H, Chen Y (2016) Promoted VOC oxidation over homogeneous porous Co_xNiAlO composite oxides derived from hydrotalcites: Effect of preparation method and doping. RSC Adv 6 (62):56874-56884. doi:10.1039/c6ra08394c
14. Zhou J, Cheng Y, Yu J, Liu G (2011) Hierarchically porous calcined lithium/aluminum layered double hydroxides: Facile synthesis and enhanced adsorption towards fluoride in water. J Mater Chem 21 (48):19353-19361. doi:10.1039/c1jm13645c
15. Li Z, Yang B, Zhang S, Wang B, Xue B (2014) A novel approach to hierarchical sphere-like ZnAl-layered double hydroxides and their enhanced adsorption capability. J Mater Chem A 2 (26):10202-10210. doi:10.1039/c4ta01028k
16. Chen L, Li C, Wei Y, Zhou G, Pan A, Wei W, Huang B (2016) Hollow LDH nanowires as excellent adsorbents for organic dye. J Alloys Compd 687:499-505. doi:10.1016/j.jallcom.2016.05.344
17. Zhou J, Yang S, Yu J, Shu Z (2011) Novel hollow microspheres of hierarchical zinc-aluminum layered double hydroxides and their enhanced adsorption capacity for phosphate in water. J Hazard Mater 192 (3):1114-1121. doi:10.1016/j.jhazmat.2011.06.013
18. Faour A, Mousty C, Prevot V, Devouard B, De Roy A, Bordet P, Elkaim E, Taviot-Gueho C (2012) Correlation among Structure, Microstructure, and Electrochemical Properties of $NiAlCO_3$ Layered Double Hydroxide Thin Films. J Phys Chem C 116 (29):15646-15659. doi:10.1021/jp300780w
19. Prevot V, Caperra N, Taviot-Gueho C, Forano C (2009) Glycine-Assisted Hydrothermal Synthesis of NiAl-Layered Double Hydroxide Nanostructures. Cryst. Growth Des. 9(8): 3646-4654.
20. Tokudome Y, Morimoto T, Tarutani N, Vaz PD, Nunes CD, Prevot V, Stenning GBG, Takahashi M (2016) Layered Double Hydroxide Nanoclusters: Aqueous, Concentrated, Stable, and Catalytically Active Colloids toward Green Chemistry. ACS Nano 10 (5):5550-5559. doi:10.1021/acsnano.6b02110
21. Tarutani N, Tokudome Y, Jobbágy M, Viva FA, Soler-Illia GJAA, Takahashi M (2016) Single-Nanometer-Sized Low-Valence Metal Hydroxide Crystals: Synthesis via Epoxide-Mediated Alkalinization and Assembly toward Functional Mesoporous Materials. Chem Mater 28 (16):5606-5610. doi:10.1021/acs.chemmater.6b02510
22. Liu J, Li Y, Huang X, Li G, Li Z (2008) Layered double hydroxide nano- and microstructures grown directly on metal substrates and their calcined products for application as Li-ion battery electrodes. Adv Funct Mater 18 (9):1448-1458
23. Zhang L, Wang J, Zhu J, Zhang X, San Hui K, Hui KN (2013) 3D porous layered double hydroxides grown on graphene as advanced electrochemical pseudocapacitor materials. J Mater Chem A 1 (32):9046-9053. doi:10.1039/c3ta11755c
24. Chen H, Zhang F, Fu S, Duan X (2006) *In situ* microstructure control of oriented layered double hydroxide monolayer films with curved hexagonal crystals as superhydrophobic materials. Adv Mater 18 (23):3089-3093. doi:10.1002/adma.200600615
25. Han J, Dou Y, Zhao J, Wei M, Evans DG, Duan X (2013) Flexible CoAl LDH@PEDOT Core/Shell Nanoplatelet Array for High-Performance Energy Storage. Small 9 (1):98-106. doi:10.1002/smll.201201336
26. Wang M, Bao W-J, Wang J, Wang K, Xu J-J, Chen H-Y, Xia X-H (2014) A green approach to the synthesis of novel Desert rose stone-like nanobiocatalytic system with excellent enzyme activity and stability. Sci Rep 4:6606
27. Wang Y, Dou H, Wang J, Ding B, Xu Y, Chang Z, Hao X (2016) Three-dimensional porous MXene/layered double hydroxide composite for high performance supercapacitors. J Power Sources 327:221-228. doi:http://dx.doi.org/10.1016/j.jpowsour.2016.07.062
28. Huang S, Zhu G-N, Zhang C, Tjiu WW, Xia Y-Y, Liu T (2012) Immobilization of CoAl Layered Double Hydroxides on Graphene Oxide Nanosheets: Growth Mechanism and Supercapacitor Studies. ACS Appl Mater Interfaces 4 (4):2242-2249. doi:10.1021/am300247x
29. Guo X, Xu S, Zhao L, Lu W, Zhang F, Evans DG, Duan X (2009) One-Step Hydrothermal Crystallization of a Layered Double Hydroxide/Alumina Bilayer Film on Aluminum and Its Corrosion Resistance Properties. Langmuir 25 (17):9894-9897. doi:10.1021/la901012w
30. Yue CL, Chen HY, Xu SL, Zhang FZ (2012) Controlled synthesis and investigation of the mechanism of formation of hollow hemispherical protrusions on laurate anion-intercalated Zn/Al layered double hydroxide hybrid films. J Colloid Interface Sci 385:268-273. doi: 10.1016/j.jcis.2012.06.008
31. Chen CP, Wangriya A, Buffet JC, O'Hare D (2015) Tuneable ultra high specific surface area Mg/Al-CO_3 layered double hydroxides. Dalton T 44 (37):16392-16398. doi:10.1039/c5dt02641e
32. Wang Q, O'Hare D (2013) Large-scale synthesis of highly dispersed layered double hydroxide powders containing delaminated single layer nanosheets. Chem Commun 49 (56):6301-6303. doi:10.1039/c3cc42918k
33. Gunjakar JL, Kim IY, Hwang SJ (2015) Efficient hybrid-type CO_2 adsorbents of reassembled layered double hydroxide 2D nanosheets with polyoxometalate 0D nanoclusters. Eur J Inorg Chem 2015 (7):1198-1202. doi:10.1002/ejic.201402480
34. Huang S, Peng HD, Tjiu WW, Yang Z, Zhu H, Tang T, Liu TX (2010) Assembling Exfoliated Layered Double Hydroxide (LDH) Nanosheet/Carbon Nanotube (CNT) Hybrids via Electrostatic Force and Fabricating Nylon Nanocomposites. J Phys Chem B 114 (50):16766-16772. doi: 10.1021/Jp1087256

35. Liu M, Wang T, Ma H, Fu Y, Hu K, Guan C (2014) Assembly of luminescent ordered multilayer thin-films based on oppositely-charged MMT and magnetic NiFe-LDHs nanosheets with ultra-long lifetimes. Sci Rep 4:7147. doi:10.1038/srep07147
36. Liu ZP, Ma RZ, Osada M, Iyi N, Ebina Y, Takada K, Sasaki T (2006) Synthesis, anion exchange, and delamination of Co-Al layered double hydroxide: Assembly of the exfoliated nanosheet/polyanion composite films and magneto-optical studies. J Am Chem Soc 128 (14):4872-4880. doi: 10.1021/Ja0584471
37. Osada M, Ebina Y, Takada K, Sasaki T (2006) Gigantic magneto-optical effects in multilayer assemblies of two-dimensional titania nanosheets. Adv Mater 18 (3):295-299. doi:10.1002/adma.200501810
38. Woo MA, Song MS, Kim TW, Kim IY, Ju JY, Lee YS, Kim SJ, Choy JH, Hwang SJ (2011) Mixed valence Zn-Co-layered double hydroxides and their exfoliated nanosheets with electrode functionality. J Mater Chem 21 (12):4286-4292. doi:10.1039/c0jm03430d
39. Prevot V, Forano C, Besse JP (2005) Hydrolysis in Polyol: New Route for Hybrid-Layered Double Hydroxides Preparation. Chem Mater 17 (26):6695-6701
40. Zhao Y, Li F, Zhang R, Evans DG, Duan X (2002) Preparation of Layered Double-Hydroxide Nanomaterials with a Uniform Crystallite Size Using a New Method Involving Separate Nucleation and Aging Steps. Chem Mater 14 (10):4286-4291
41. Prevot V, Szczepaniak C, Jaber M (2011) Aerosol-assisted self-assembly of hybrid Layered Double Hydroxide particles into spherical architectures. J Colloid Interface Sci 356 (2):566-572. doi:10.1016/j.jcis.2011.01.051
42. Wang Y, Zhang F, Xu S, Wang X, Evans DG, Duan X (2008) Preparation of Layered Double Hydroxide Microspheres by Spray Drying. Ind Eng Chem Res 47 (15):5746-5750. doi:10.1021/ie800146m
43. Huo R, Kuang Y, Zhao Z, Zhang F, Xu S (2013) Enhanced photocatalytic performances of hierarchical $ZnO/ZnAl_2O_4$ microsphere derived from layered double hydroxide precursor spray-dried microsphere. J Colloid Interface Sci 407:17-21. doi:http://dx.doi.org/10.1016/j.jcis.2013.06.067
44. Shi J-L, Peng H-J, Zhu L, Zhu W, Zhang Q (2015) Template growth of porous graphene microspheres on layered double oxide catalysts and their applications in lithium sulfur batteries. Carbon 92:96-105. doi:http://dx.doi.org/10.1016/j.carbon.2015.03.031
45. Pierre AC, Pajonk GM (2002) Chemistry of Aerogels and their applications. Chem Rev 102:4243-4265
46. Tokudome Y, Fukui M, Tarutani N, Nishimura S, Prevot V, Forano C, Poologasundarampillai G, Lee PD, Takahashi M (2016) High-Density Protein Loading on Hierarchically Porous Layered Double Hydroxide Composites with a Rational Mesostructure. Langmuir 32 (35):8826-8833. doi:10.1021/acs.langmuir.6b01925
47. Touati S, Mansouri H, Benguedach A, de Roy A, Forano C, Prevot V (2012) Nanostructured layered double hydroxide aerogels with enhanced adsorption properties. Chem Commun 48 (57):7197-7199. doi: 10.1039/C2cc31817b
48. Hu Z, Chen G (2014) Novel nanocomposite hydrogels consisting of layered double hydroxide with ultrahigh tensibility and hierarchical porous structure at low inorganic content. Adv Mater 26 (34):5950-5956. doi:10.1002/adma.201400179
49. Shafiei SS, Shavandi M, Ahangari G, Shokrolahi F (2016) Electrospun layered double hydroxide/poly (ε-caprolactone) nanocomposite scaffolds for adipogenic differentiation of adipose-derived mesenchymal stem cells. Appl Clay Sci 127-128:52-63. doi:10.1016/j.clay.2016.04.004
50. Gomez-Fernandez S, Ugarte L, Pena-Rodriguez C, Zubitur M, Corcuera MA, Eceiza A (2016) Flexible polyurethane foam nanocomposites with modified layered double hydroxides. Appl Clay Sci 123:109-120. doi:http://dx.doi.org/10.1016/j.clay.2016.01.015
51. Martinez AB, Realinho V, Antunes M, Maspoch ML, Velasco JI (2011) Microcellular Foaming of Layered Double Hydroxide Polymer Nanocomposites. Ind Eng Chem Res 50 (9):5239-5247. doi:10.1021/ie101375f
52. Zhang A, Wang C, Xu Q, Liu H, Wang Y, Xia Y (2015) A hybrid aerogel of Co-Al layered double hydroxide/graphene with three-dimensional porous structure as a novel electrode material for supercapacitors. RSC Adv 5 (33):26017-26026. doi:10.1039/c5ra00103j
53. Soler-Illia GJDAA, Sanchez C, Lebeau B, Patarin J (2002) Chemical strategies to design textured materials: From microporous and mesoporous oxides to nanonetworks and hierarchical structures. Chem Rev 102 (11):4093-4138. doi:10.1021/cr0200062
54. Torchilin VP (2007) Micellar nanocarriers: Pharmaceutical perspectives. Pharm Res 24 (1):1-16. doi:10.1007/s11095-006-9132-0
55. Wong MS, Jeng ES, Ying JY (2001) Supramolecular Templating of Thermally Stable Crystalline Mesoporous Metal Oxides Using Nanoparticulate Precursors. Nano Lett 1 (11):637-642. doi:10.1021/nl015594y
56. Chane-Ching JY, Cobo F, Aubert D, Harvey HG, Airiau M, Corma A (2005) A general method for the synthesis of nanostructured large-surface-area materials through the self-assembly of functionalized nanoparticles. Chem - A Eur J 11 (3):979-987. doi:10.1002/chem.200400535
57. Inagaki S, Guan S, Ohsuna T, Terasaki O (2002) An ordered mesoporous organosilica hybrid material with a crystal-like wall structure. Nature 416 (6878):304-307. doi:10.1038/416304a

58. Choi M, Cho HS, Srivastava R, Venkatesan C, Choi DH, Ryoo R (2006) Amphiphilic organosilane-directed synthesis of crystalline zeolite with tunable mesoporosity. Nat Mater 5 (9):718-723. doi:10.1038/nmat1705
59. Wu Z, Li Q, Feng D, Webley PA, Zhao D (2010) Ordered mesoporous crystalline γ-Al_2O_3 with variable architecture and porosity from a single hard template. J Am Chem Soc 132 (34):12042-12050. doi:10.1021/ja104379a
60. Tang J, Wu Y, McFarland EW, Stucky GD (2004) Synthesis and photocatalytic properties of highly crystalline and ordered mesoporous TiO_2 thin films. Chem Commun 10 (14):1670-1671
61. Gunawan P, Xu R (2008) Synthesis of unusual coral-like layered double hydroxide microspheres in a nonaqueous polar solvent/surfactant system. J Mater Chem 18 (18):2112-2120. doi:10.1039/b719817e
62. Zhang J, Xie X, Li C, Wang H, Wang L (2015) The role of soft colloidal templates in the shape evolution of flower-like MgAl-LDH hierarchical microstructures. RSC Adv 5 (38):29757-29765. doi:10.1039/c5ra01561h
63. Sun H, Chu Z, Hong D, Zhang G, Xie Y, Li L, Shi K (2016) Three-dimensional hierarchical flower-like Mg-Al-layered double hydroxides: Fabrication, characterization and enhanced sensing properties to NO_x at room temperature. J Alloys Compd 658:561-568. doi:10.1016/j.jallcom.2015.10.237
64. Shao M, Ning F, Zhao J, Wei M, Evans DG, Duan X (2013) Hierarchical layered double hydroxide microspheres with largely enhanced performance for ethanol electrooxidation. Adv Funct Mater 23 (28):3513-3518. doi:10.1002/adfm.201202825
65. Wu X, Jiang L, Long C, Wei T, Fan Z (2015) Dual Support System Ensuring Porous Co-Al Hydroxide Nanosheets with Ultrahigh Rate Performance and High Energy Density for Supercapacitors. Adv Funct Mater 25 (11):1648-1655. doi:10.1002/adfm.201404142
66. Oestreicher V, Jobbagy M (2013) One Pot Synthesis of $Mg_2Al(OH)_6Cl{\cdot}1.5H_2O$ Layered Double Hydroxides: The Epoxide Route. Langmuir 29 (39):12104-12109. doi: 10.1021/La402260m
67. Gash AE, Tillotson TM, Satcher JH, Poco JF, Hrubesh LW, Simpson RL (2001) Use of epoxides in the sol-gel synthesis of porous iron(III) oxide monoliths from Fe(III) salts. Chem Mater 13 (3):999-1007. doi: 10.1021/Cm0007611
68. Tokudome Y, Fujita K, Nakanishi K, Miura K, Hirao K (2007) Synthesis of Monolithic Al_2O_3 with Well-Defined Macropores and Mesostructured Skeletons via the Sol-Gel Process Accompanied by Phase Separation. Chem Mater 19:3393-3398. doi: 10.1021/cm063051p
69. Tokudome Y, Tarutani N, Nakanishi K, Takahashi M (2013) Layered double hydroxide (LDH)-based monolith with interconnected hierarchical channels: enhanced sorption affinity for anionic species. J Mater Chem A 1 (26):7702-7708. doi: 10.1039/C3ta11110e
70. Tarutani N, Tokudome Y, Fukui M, Nakanishi K, Takahashi M (2015) Fabrication of hierarchically porous monolithic layered double hydroxide composites with tunable microcages for effective oxyanion adsorption. RSC Adv 5 (70):57187-57192. doi:10.1039/c5ra05942a
71. Han J, Dou Y, Wei M, Evans DG, Duan X (2010) Erasable nanoporous antireflection coatings based on the reconstruction effect of layered double hydroxides. Angew Chem Int Ed 49 (12):2171-2174. doi:10.1002/anie.200907005
72. Jiang S-D, Song L, Zeng W-R, Huang Z-Q, Zhan J, Stec AA, Hull TR, Hu Y, Hu W-Z (2015) Self-Assembly Fabrication of Hollow Mesoporous Silica@CoAl Layered Double Hydroxide@Graphene and Application in Toxic Effluents Elimination. ACS Appl Mater Interfaces 7 (16):8506-8514. doi:10.1021/acsami.5b00176
73. Yan Q, Zhang Z, Zhang Y, Umar A, Guo Z, O'Hare D, Wang Q (2015) Hierarchical Fe_3O_4 Core–Shell Layered Double Hydroxide Composites as Magnetic Adsorbents for Anionic Dye Removal from Wastewater. Eur J Inorg Chem 2015 (25):4182-4191. doi:10.1002/ejic.201500650
74. Basile F, Benito P, Fornasari G, Rosetti V, Scavetta E, Tonelli D, Vaccari A (2009) Electrochemical synthesis of novel structured catalysts for H_2 production. Appl Catal, B 91 (1-2):563-572. doi:http://dx.doi.org/10.1016/j.apcatb.2009.06.028
75. Lai F, Huang Y, Miao Y-E, Liu T (2015) Controllable preparation of multi-dimensional hybrid materials of nickel-cobalt layered double hydroxide nanorods/nanosheets on electrospun carbon nanofibers for high-performance supercapacitors. Electrochim Acta 174:456-463. doi:http://dx.doi.org/10.1016/j.electacta.2015.06.031
76. Abushrenta N, Wu X, Wang J, Liu J, Sun X (2015) Hierarchical Co-based Porous Layered Double Hydroxide Arrays Derived via Alkali Etching for High-performance Supercapacitors. Sci Rep 5:13082, doi:10.1038/srep13082
77. Xie R, Fan G, Yang L, Li F (2016) Hierarchical flower-like Co-Cu mixed metal oxide microspheres as highly efficient catalysts for selective oxidation of ethylbenzene. Chem. Eng. J. 288:169-178. doi:http://dx.doi.org/10.1016/j.cej.2015.12.004
78. Zhang F, Chen J, Chen P, Sun Z, Xu S (2012) Pd nanoparticles supported on hydrotalcite-modified porous alumina spheres as selective hydrogenation catalyst. AIChE J 58 (6):1853-1861. doi:10.1002/aic.12694
79. Liu M, He S, Miao Y-E, Huang Y, Lu H, Zhang L, Liu T (2015) Eco-friendly synthesis of hierarchical ginkgo-derived carbon nanoparticles/NiAl-layered double hydroxide hybrid electrodes toward high-performance

supercapacitors. RSC Adv 5 (68):55109-55118. doi:10.1039/c5ra07215h
80. Zhang T, Mei ZY, Zhou YM, Yu SN, Chen ZJ, Bu XH (2014) Novel paper-templated fabrication of hierarchically porous Ni-Al layered double hydroxides/Al_2O_3 for efficient BSA separation. J Chem Technol Biotechnol 89 (11):1705-1711. doi: 10.1002/Jctb.4248
81. Zhang T, Zhou Y, He M, Bu X, Wang Y, Zhang C (2015) Templated fabrication of biomorphic alumina-based ceramics with hierarchical structure. J Eur Ceram Soc 35 (4):1337-1341. doi:10.1016/j.jeurceramsoc.2014.10.029
82. Jia Z, Wang Y, Qi T (2015) Hierarchical Ni-Fe layered double hydroxide/MnO_2 sphere architecture as an efficient noble metal-free electrocatalyst for ethanol electro-oxidation in alkaline solution. RSC Adv 5 (101):83314-83319. doi:10.1039/c5ra15718h
83. Zhang H, Zhang G, Bi X, Chen X (2013) Facile assembly of a hierarchical core@shell Fe_3O_4@CuMgAl-LDH (layered double hydroxide) magnetic nanocatalyst for the hydroxylation of phenol. J Mater Chem A 1 (19):5934-5942. doi:10.1039/c3ta10349h
84. Yin S, Li J, Zhang H (2016) Hierarchical hollow nanostructured core@shell recyclable catalysts γ-Fe_2O_3@LDH@Au25-x for highly efficient alcohol oxidation. Green Chem 18 (21):5900-5914. doi:10.1039/c6gc01290f
85. Badar M, Rahim MI, Kieke M, Ebel T, Rohde M, Hauser H, Behrens P, Mueller PP (2015) Controlled drug release from antibiotic-loaded layered double hydroxide coatings on porous titanium implants in a mouse model. J Biomed Materi Res, Part A 103 (6):2141-2149. doi:10.1002/jbm.a.35358
86. Chen H, Hu L, Chen M, Yan Y, Wu L (2014) Nickel-cobalt layered double hydroxide nanosheets for high-performance supercapacitor electrode materials. Adv Funct Mater 24 (7):934-942. doi:10.1002/adfm.201301747
87. Chen C, Byles CFH, Buffet J-C, Rees NH, Wu Y, O'Hare D (2016) Core-shell zeolite@aqueous miscible organic-layered double hydroxides. Chem Sci 7 (2):1457-1461. doi:10.1039/c5sc03208c
88. Gomez-Aviles A, Aranda P, Ruiz-Hitzky E (2016) Layered double hydroxide/sepiolite heterostructured materials. Appl Clay Sci 130:83-92. doi: http:// dx.doi.org/10.1016/j.clay.2015.12.011
89. Tian N, Tian X, Liu X, Zhou Z, Yang C, Ma L, Tian C, Li Y, Wang Y (2016) Facile synthesis of hierarchical dendrite-like structure iron layered double hydroxide nanohybrids for effective arsenic removal. Chem Commun 52 (80):11955-11958. doi:10.1039/c6cc05659h
90. Jia G, Hu Y, Qian Q, Yao Y, Zhang S, Li Z, Zou Z (2016) Formation of Hierarchical Structure Composed of (Co/Ni)Mn-LDH Nanosheets on MWCNT Backbones for Efficient Electrocatalytic Water Oxidation. ACS Appl Mater Interfaces 8 (23):14527-14534. doi:10.1021/acsami.6b02733
91. Mandal S, Mayadevi S (2008) Cellulose supported layered double hydroxides for the adsorption of fluoride from aqueous solution. Chemosphere 72 (6):995-998. doi:http://dx.doi.org/10.1016/j.chemosphere.2008.03.053
92. Sobhana SSL, Bogati DR, Reza M, Gustafsson J, Fardim P (2016) Cellulose biotemplates for layered double hydroxides networks. Microporous Mesoporous Mater 225:66-73. doi:10.1016/j.micromeso.2015.12.009
93. Wu S, Hui KS, Hui KN (2015) One-Dimensional Core-Shell Architecture Composed of Silver Nanowire@Hierarchical Nickel Aluminum Layered Double Hydroxide Nanosheet as Advanced Electrode Materials for Pseudocapacitor. J Phys Chem C 119 (41):23358-23365. doi:10.1021/acs.jpcc.5b07739
94. Liu X, Tian W, Kong X, Jiang M, Sun X, Lei X (2015) Selective removal of thiosulfate from thiocyanate-containing water by a three-dimensional structured adsorbent: A calcined NiAl-layered double hydroxide film. RSC Adv 5 (107):87948-87955. doi:10.1039/c5ra14127c
95. Guoxiang P, Xinhui X, Jingshan L, Feng C, Zhihong Y, Hongjin F (2014) Preparation of CoAl layered double hydroxide nanoflake arrays and their high supercapacitance performance. Appl Clay Sci 102:28-32. doi:http://dx.doi.org/10.1016/j.clay.2014.10.003
96. Yang Q, Li T, Lu Z, Sun X, Liu J (2014) Hierarchical construction of an ultrathin layered double hydroxide nanoarray for highly-efficient oxygen evolution reaction. Nanoscale 6 (20):11789-11794. doi:10.1039/c4nr03371j
97. Tian W, Kong X, Jiang M, Lei X, Duan X (2016) Hierarchical layered double hydroxide epitaxially grown on vermiculite for Cr(VI) removal. Mater Lett 175:110-113. doi:10.1016/j.matlet.2016.03.141
98. Yan L, Li R, Li Z, Liu J, Fang Y, Wang G, Gu Z (2013) Three-dimensional activated reduced graphene oxide nanocup/nickel aluminum layered double hydroxides composite with super high electrochemical and capacitance performances. Electrochim Acta 95:146-154. doi:http://dx.doi.org/10.1016/j.electacta.2013.02.060
99. Wan H, Liu J, Ruan Y, Lv L, Peng L, Ji X, Miao L, Jiang J (2015) Hierarchical Configuration of $NiCo_2S_4$ Nanotube@Ni-Mn Layered Double Hydroxide Arrays/Three-Dimensional Graphene Sponge as Electrode Materials for High-Capacitance Supercapacitors. ACS Appl Mater Interfaces 7 (29):15840-15847. doi:10.1021/acsami.5b03042
100. Ma K, Cheng JP, Liu F, Zhang X (2016) Co-Fe layered double hydroxides nanosheets vertically grown on carbon fiber cloth for electrochemical capacitors. J Alloys Compd 679:277-284. doi:10.1016/j.jallcom.2016.04.059
101. Zhao J, Lu Z, Shao M, Yan D, Wei M, Evans DG, Duan X (2013) Flexible hierarchical nanocomposites

based on MnO_2 nanowires/CoAl hydrotalcite/carbon fibers for high-performance supercapacitors. RSC Adv 3 (4):1045-1049. doi:10.1039/c2ra22566b
102. Yu J, Lu L, Li J, Song P (2016) Biotemplated hierarchical porous-structure of ZnAl-LDH/$ZnCo_2O_4$ composites with enhanced adsorption and photocatalytic performance. RSC Adv 6 (16):12797-12808. doi:10.1039/c5ra15758g
103. Sailaja GS, Zhang P, Anilkumar GM, Yamaguchi T (2015) Aniosotropically Organized LDH on PVDF: A Geometrically Templated Electrospun Substrate for Advanced Anion Conducting Membranes. ACS Appl Mater Interfaces 7 (12):6397-6401. doi:10.1021/acsami.5b00532
104. Shami Z, Amininasab SM, Shakeri P (2016) Structure-Property Relationships of Nanosheeted 3D Hierarchical Roughness MgAl-Layered Double Hydroxide Branched to an Electrospun Porous Nanomembrane: A Superior Oil-Removing Nanofabric. ACS Appl Mater Interfaces 8 (42):28964-28973. doi:10.1021/acsami.6b07744
105. Li Z, Shao M, Zhou L, Zhang R, Zhang C, Han J, Wei M, Evans DG, Duan X (2016) A flexible all-solid-state micro-supercapacitor based on hierarchical CuO@layered double hydroxide core shell nanoarrays. Nano Energy 20:294-304. doi:http://dx.doi.org/10.1016/j.nanoen.2015.12.030
106. Fan X, Gao B, Wang T, Huang X, Gong H, Xue H, Guo H, Song L, Xia W, He J (2016) Layered double hydroxide modified WO_3 nanorod arrays for enhanced photoelectrochemical water splitting. Appl Catal, A 528:52-58. doi:http://dx.doi.org/10.1016/j.apcata.2016.09.014
107. Benito P, de Nolf W, Nuyts G, Monti M, Fornasari G, Basile F, Janssens K, Ospitali F, Scavetta E, Tonelli D, Vaccari A (2014) Role of Coating-Metallic Support Interaction in the Properties of Electrosynthesized Rh-Based Structured Catalysts. ACS Catal 4 (10):3779-3790. doi:10.1021/cs501079k
108. Lu X, Zhao C (2015) Electrodeposition of hierarchically structured three-dimensional nickel iron electrodes for efficient oxygen evolution at high current densities. Nat Commun 6:6616
109. Li Z, Shao M, An H, Wang Z, Xu S, Wei M, Evans DG, Duan X (2015) Fast electrosynthesis of Fe-containing layered double hydroxide arrays toward highly efficient electrocatalytic oxidation reactions. Chem Sci 6 (11):6624-6631. doi:10.1039/c5sc02417j
110. Shao M, Li Z, Zhang R, Ning F, Wei M, Evans DG, Duan X (2015) Hierarchical Conducting Polymer@Clay Core–Shell Arrays for Flexible All-Solid-State Supercapacitor Devices. Small 11 (29):3530-3538. doi:10.1002/smll.201403421
111. Shao M, Ning F, Zhao J, Wei M, Evans DG, Duan X (2012) Preparation of Fe_3O_4@SiO_2@Layered Double Hydroxide Core-Shell Microspheres for Magnetic Separation of Proteins. J Am Chem Soc 134 (2):1071-1077. doi:10.1021/ja2086323
112. Zhang T, Zhou Y, Bu X, Wang Y, Qiu F (2015) Controlled fabrication of hierarchical $MgAl_2O_4$ spinel/carbon fiber composites by crystal growth and calcination processes. Ceram Int 41 (9, Part B):12504-12508. doi:http://dx.doi.org/10.1016/j.ceramint.2015.05.130
113. Zhang T, Zhou Y, Wang Y, Bu X, Wang H, Zhang M (2015) Morphology-controlled fabrication of hierarchical LDH/C microspheres derived from rape pollen grain. Appl Clay Sci 103:67-70. doi:10.1016/j.clay.2014.11.012
114. Du X, Zhang D, Shi L, Gao R, Zhang J (2013) Coke- and sintering-resistant monolithic catalysts derived from *in situ* supported hydrotalcite-like films on Al wires for dry reforming of methane. Nanoscale 5 (7):2659-2663. doi:10.1039/c3nr33921a
115. Ghani M, Frizzarin RM, Maya F, Cerda V (2016) In-syringe extraction using dissolvable layered double hydroxide-polymer sponges templated from hierarchically porous coordination polymers. J Chromatogr A 1453:1-9. doi:http://dx.doi.org/10.1016/j.chroma.2016.05.023
116. Chang YP, Chen YC, Chang PH, Chen SY (2012) Synthesis, characterization, and CO_2 adsorptive behavior of mesoporous AlOOH-supported layered hydroxides. ChemSusChem 5 (7):1249-1257. doi:10.1002/cssc.201100617
117. Yue Y, Liu F, Zhao L, Zhang L, Liu Y (2015) Loading oxide nano sheet supported NiCo alloy nanoparticles on the macroporous walls of monolithic alumina and their catalytic performance for ethanol steam reforming. Int J Hydrogen Energy 40 (22):7052-7063. doi:http://dx.doi.org/10.1016/j.ijhydene.2015.04.036
118. Li L, Shi J (2008) *In situ* assembly of layered double hydroxide nano-crystallites within silica mesopores and its high solid base catalytic activity. Chem Commun (8):996-998. doi:10.1039/b717876j
119. Creasey JJ, Parlett CMA, Manayil JC, Isaacs MA, Wilson K, Lee AF (2015) Facile route to conformal hydrotalcite coatings over complex architectures: a hierarchically ordered nanoporous base catalyst for FAME production. Green Chem 17 (4):2398-2405. doi:10.1039/c4gc01689k
120. Zhang T, Mei Z, Zhou Y, Bu X, Wang Y, Li Q, Yang X (2014) Template-controlled fabrication of hierarchical porous Zn-Al composites with tunable micro/nanostructures and chemical compositions. Cryst Eng Comm 16 (9):1793-1801. doi:10.1039/c3ce41839a
121. Zhang T, Zhou Y, Bu X, Xue J, Hu J, Wang Y, Zhang M (2014) Bio-inspired fabrication of hierarchically porous Mg-Al composites for enhanced BSA adsorption properties. Microporous Mesoporous Mater 188:37-45.

doi:10.1016/j.micromeso.2014.01.001
122. Hai B, Zou Y (2015) Carbon cloth supported NiAl-layered double hydroxides for flexible application and highly sensitive electrochemical sensors. Sens Actuators, B 208:143-150. doi:http://dx.doi.org/10.1016/j.snb.2014.11.022
123. Kim TW, Sahimi M, Tsotsis TT (2008) Preparation of Hydrotalcite Thin Films Using an Electrophoretic Technique. Ind Eng Chem Res 47 (23):9127-9132. doi:10.1021/ie071446s
124. Ma W, Meng F, Cheng Z, Sha X, Xin G, Tan D (2015) Synthesized of macroporous composite electrode by activated carbon fiber and MgCaAl (NO_3) hydrotalcite-like compounds to remove bromate. Colloids Surf A 481:393-399. doi:http://dx.doi.org/10.1016/j.colsurfa.2015.06.004
125. Liu L, Wang W, Hu Y (2015) Layered double hydroxide-decorated flexible polyurethane foam: significantly improved toxic effluent elimination. RSC Adv 5 (118):97458-97466. doi:10.1039/c5ra19414h
126. Shao M, Ning F, Zhao Y, Zhao J, Wei M, Evans DG, Duan X (2012) Core Shell Layered Double Hydroxide Microspheres with Tunable Interior Architecture for Supercapacitors. Chem Mater 24 (6):1192-1197. doi:10.1021/cm203831p
127. Zhang C, Shao M, Zhou L, Li Z, Xiao K, Wei M (2016) Hierarchical NiFe Layered Double Hydroxide Hollow Microspheres with Highly-Efficient Behavior toward Oxygen Evolution Reaction. ACS Appl Mater Interfaces. doi:10.1021/acsami.6b12100
128. Gunawan P, Xu R (2009) Direct assembly of anisotropic layered double hydroxide (LDH) nanocrystals on spherical template for fabrication of drug-LDH hollow nanospheres. Chem Mater 21 (5):781-783. doi:10.1021/cm803203x
129. Xu J, He F, Gai S, Zhang S, Li L, Yang P (2014) Nitrogen-enriched, double-shelled carbon/layered double hydroxide hollow microspheres for excellent electrochemical performance. Nanoscale 6 (18):10887-10895. doi:10.1039/c4nr02756f
130. Li J, Zhang N, Ng DHL (2015) Synthesis of a 3D hierarchical structure of γ-AlO(OH)/Mg-Al-LDH/C and its performance in organic dyes and antibiotics adsorption. J Mater Chem A 3 (42):21106-21115. doi:10.1039/c5ta04497a
131. Zhang F, Xie Y, Xu S, Zhao X, Lei X (2010) Facile Fabrication and Magnetic Properties of Macroporous Spinel Microspheres from Layered Double Hydroxide Microsphere Precursor. Chem Lett 39 (6):588-590. doi: 10.1246/cl.2010.588
132. Li L, Ma R, Iyi N, Ebina Y, Takada K, Sasaki T (2006) Hollow nanoshell of layered double hydroxide. Chem Commun (29):3125-3127. doi:10.1039/b605889b
133. Martin J, Jack M, Hakimian A, Vaillancourt N, Villemure G (2016) Electrodeposition of Ni-Al layered double hydroxide thin films having an inversed opal structure: Application as electrochromic coatings. J Electroanal Chem 780:217-224. doi:http://dx.doi.org/10.1016/j.jelechem.2016.09.022
134. Prevot V, Forano C, Khenifi A, Ballarin B, Scavetta E, Mousty C (2011) A templated electrosynthesis of macroporous NiAl layered double hydroxides thin films. Chem Commun 47 (6):1761-1763. doi:10.1039/c0cc04255b
135. Abolghasemi MM, Yousefi V (2014) Three dimensionally honeycomb layered double hydroxides framework as a novel fiber coating for headspace solid-phase microextraction of phenolic compounds. J Chromatogr A 1345:9-16. doi:10.1016/j.chroma.2014.04.018
136. Da Silva ES, Prevot V, Forano C, Wong-Wah-Chung P, Burrows HD, Sarakha M (2014) Heterogeneous photocatalytic degradation of pesticides using decatungstate intercalated macroporous layered double hydroxides. Environ Sci Pollut Res 21 (19):11218-11227. doi:10.1007/s11356-014-2971-z
137. Geraud E, Bouhent M, Derriche Z, Leroux F, Prevot V, Forano C (2007) Texture effect of layered double hydroxides on chemisorption of Orange II. J Phys Chem Solids 68 (5-6):818-823. doi:http://dx.doi.org/10.1016/j.jpcs.2007.02.053
138. Geraud E, Prevot V, Ghanbaja J, Leroux F (2006) Macroscopically Ordered Hydrotalcite-Type Materials Using Self-Assembled Colloidal Crystal Template. Chem Mater 18 (2):238-240. doi:10.1021/cm051770i
139. Geraud E, Rafqah S, Sarakha M, Forano C, Prevot V, Leroux F (2008) Three dimensionally ordered macroporous layered double hydroxides: Preparation by templated impregnation/coprecipitation and pattern stability upon calcination. Chem Mater 20 (3):1116-1125. doi: 10.1021/Cm702755h
140. Halma M, Castro KADdF, Prevot V, Forano C, Wypych F, Nakagaki S (2009) Immobilization of anionic iron(III) porphyrins into ordered macroporous layered double hydroxides and investigation of catalytic activity in oxidation reactions. J Mol Catal A: Chem 310 (1-2):42-50. doi:http://dx.doi.org/10.1016/j.molcata.2009.05.017
141. Woodford JJ, Dacquin J-P, Wilson K, Lee AF (2012) Better by design: nanoengineered macroporous hydrotalcites for enhanced catalytic biodiesel production. Energy Environ Sci 5 (3):6145-6150. doi:10.1039/c2ee02837a
142. Zhao YF, Wei M, Lu J, Wang ZL, Duan X (2009) Biotemplated Hierarchical Nanostructure of Layered Double Hydroxides with Improved Photocatalysis Performance. ACS Nano 3 (12):4009-4016. doi:

10.1021/Nn901055d
143. Xiang X, Hima HI, Wang H, Li F (2008) Facile synthesis and catalytic properties of nickel-based mixed-metal oxides with mesopore networks from a novel hybrid composite precursor. Chem Mater 20 (3):1173-1182. doi:10.1021/cm702072t
144. Chen C, Felton R, Buffet J-C, O'Hare D (2015) Core-shell SiO_2@LDHs with tuneable size, composition and morphology. Chem Commun 51 (16):3462-3465. doi:10.1039/c4cc10008e
145. Tarutani N, Tokudome Y, Nakanishi K, Takahashi M (2014) Layered double hydroxide composite monoliths with three-dimensional hierarchical channels: structural control and adsorption behavior. RSC Adv 4 (31):16075-16080. doi: 10.1039/C4ra00873a
146. Lei C, Zhu X, Zhu B, Jiang C, Le Y, Yu J (2017) Superb adsorption capacity of hierarchical calcined Ni/Mg/Al layered double hydroxides for Congo red and Cr(VI) ions. J Hazard Mater 321:801-811. doi:10.1016/j.jhazmat.2016.09.070
147. Varadwaj GBB, Nyamori VO (2016) Layered double hydroxide- and graphene-based hierarchical nanocomposites: Synthetic strategies and promising applications in energy conversion and conservation. Nano Res 9 (12):3598-3621. doi:10.1007/s12274-016-1250-3
148. Wang Y, Cao D, Wang G, Wang S, Wen J, Yin J (2011) Spherical clusters of β-$Ni(OH)_2$ nanosheets supported on nickel foam for nickel metal hydride battery. Electrochim Acta 56 (24):8285-8290. doi:10.1016/j.electacta.2011.06.098
149. Liu X, Wang X, Yuan X, Dong W, Huang F (2015) Rational composition and structural design of *in situ* grown nickel-based electrocatalysts for efficient water electrolysis. J Mater Chem A 4 (1):167-172. doi:10.1039/c5ta07047c
150. Liang H, Li L, Meng F, Dang L, Zhuo J, Forticaux A, Wang Z, Jin S (2015) Porous Two-Dimensional Nanosheets Converted from Layered Double Hydroxides and Their Applications in Electrocatalytic Water Splitting. Chem Mater 27 (16):5702-5711. doi:10.1021/acs.chemmater.5b02177
151. Charradi K, Forano C, Prevot V, Madern D, Amara ABH, Mousty C (2010) Characterization of hemoglobin immobilized in MgAl-layered double hydroxides by the coprecipitation method. Langmuir 26 (12):9997-10004